Aalborg Universitet

AALBORG UNIVERSITY
DENMARK

Investigation of Heat Transfer in Mini Channels using Planar Laser Induced Fluorescence

Bøgild, Morten Ryge; Poulsen, Jonas Lundsted; Rath, Emil Zacho; Sørensen, Henrik

Published in:
Proceedings of 6th European Thermal Sciences Conference (Eurotherm 2012)

DOI (link to publication from Publisher):
10.1088/1742-6596/395/1/012080

Publication date:
2012

Document Version
Early version, also known as pre-print

Link to publication from Aalborg University

Citation for published version (APA):
Bøgild, M. R., Poulsen, J. L., Rath, E. Z., & Sørensen, H. (2012). Investigation of Heat Transfer in Mini Channels using Planar Laser Induced Fluorescence. In D. Petit, & C. L. Niliot (Eds.), *Proceedings of 6th European Thermal Sciences Conference (Eurotherm 2012)* (pp. Article No. 012080). IOP Publishing. https://doi.org/10.1088/1742-6596/395/1/012080

General rights
Copyright and moral rights for the publications made accessible in the public portal are retained by the authors and/or other copyright owners and it is a condition of accessing publications that users recognise and abide by the legal requirements associated with these rights.

- Users may download and print one copy of any publication from the public portal for the purpose of private study or research.
- You may not further distribute the material or use it for any profit-making activity or commercial gain
- You may freely distribute the URL identifying the publication in the public portal -

Take down policy
If you believe that this document breaches copyright please contact us at vbn@aub.aau.dk providing details, and we will remove access to the work immediately and investigate your claim.

Investigation of Heat Transfer in Mini Channels using Planar Laser Induced Fluorescence

M R Bøgild, J L Poulsen, E Z Rath, and H Sørensen

Department of Energy, Aalborg University, Pontoppidanstræde 101, 9000 Aalborg, Denmark

E-mail: jonas.lundsted@gmail.com

Abstract. In this paper an experimental investigation of the heat transfer in mini channels with a hydraulic diameter of 889 μm is conducted. The method used is planar laser induced fluorescence (PLIF), which uses the principle of laser excitation of rhodamine B in water. The goal of this study is to validate the applicability of PLIF to determine the convective heat transfer coefficient in mini channels against conventional correlations of the convective heat transfer coefficient. The applicability of the conventional theory in micro and mini channels has been discussed by several researchers, but to the authors knowledge the applicability of PLIF to validate this has not yet been investigated thoroughly. The experiment shows good agreement to the conventional correlation, and the resolution of the temperature gradient at the wall is found sufficiently accurate in certain areas. However, PLIF is not found satisfactory over the whole domain, and the limitations and errors are analysed.

1. Introduction

Investigation of the micro scale heat transfer is a relevant topic due to the question of the applicability of conventional heat transfer correlations. The published results of the various studies diverse from one another. The convective heat transfer coefficient has either fallen below [1] or above [2, 3] the value expected for conventional length scale channels. Others have reported little, or no diversity from conventional length scales [4]. In the present study the goal is to use the non-intrusive method of planer laser induced fluorescence (PLIF) for determination of local temperatures in mini channels with a hydraulic diameter of 889 μm. With this method it should be possible to find the temperature gradient at the wall, which can be used to find the convective heat transfer coefficient [5]:

$$h = \frac{-k_{fluid}\,(\partial T/\partial y)_{y=0}}{T_{wall} - T_{\infty}} \qquad \left[\frac{W}{m^2 K}\right] \tag{1}$$

h is the convective heat transfer coefficient, k_{fluid} is the conductive heat transfer coefficient of the fluid, $(\partial T/\partial y)_{y=0}$ is the temperature gradient at the wall, T_{wall} is the temperature at the wall and T_{∞} is the temperature of the water sufficiently far from the wall. The above equation is valid because the fluid adjacent to the wall is motionless as a consequence of the no-slip condition, and hence the conductive heat transfer per area is equal to the convective heat transfer per area. By using PLIF to find the temperature gradient it may be possible to validate the above statements. The goal of the present paper is to investigate the applicability of PLIF to determine the convective heat transfer coefficient.

Figure 1 (a) shows the dimensions of the mini channels used for the experiment. The length of the module is the same as the width. For this specific case the cross sectional aspect ratio of the channels is 8, and the length of each of the 19 channels is 20 mm. The hydraulic diameter is 889 μm. Figure 1 (b) shows the experimental setup with laser, camera, and flow box containing the mini channels.

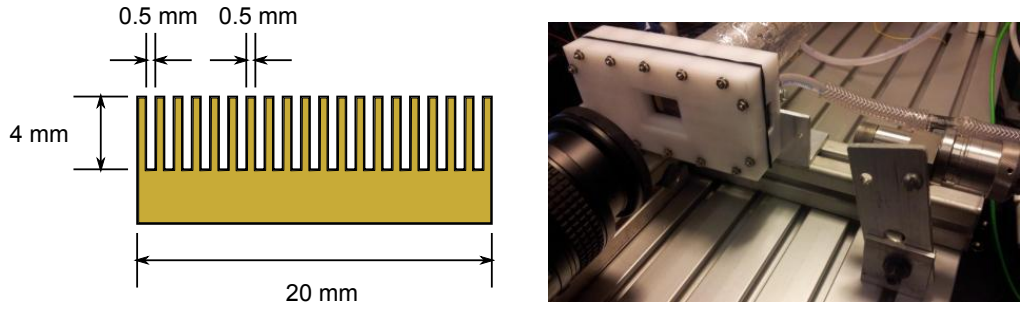

(a) (b)

Figure 1. *Figure (a) showing channel dimensions, and figure (b) showing experimental setup.*

In the present paper an experiment is conducted with a flow of 0.5 l/min, corresponding to a Reynolds number of 260, and the heat input power is 100 W.

2. Conventional Nusselt Number Approximation

The conventional heat transfer theory does in many cases not apply to a specific problem, often because the specific problem is too complex. Thus, the problem needs to be simplified, or to be divided into parts where different theory applies. The theory of flow in mini channels corresponds to the theory of either forced convection in ducts, or forced convection between two parallel plates due to a high aspect ratio. The Nusselt number depends on these assumptions. The flow in mini channels is in this case kept in the laminar regime, which develops through the channel. Several different cases of flow are described by the conventional theory, where both the hydrodynamical and thermal boundary layer can be assumed to be either fully developed or developing. These assumptions can then be combined in a variety of ways.

The Nusselt number theory is often divided into two cases; the walls have constant temperature or the heat flux is constant through the channel. None of the two cases apply perfectly, but the case of constant heat flux is the best compromise between the two cases.

Since the hydrodynamical boundary layer is developing until $L_H = 0.05ReD_h$ for laminar flow, a Reynolds number of more than 450 leads to a developing flow throughout the full channel length. The correlation of Stephan and Preusser [6] describes simultaneously developing flow with constant wall heat flux in circular geometry, and do not account for aspect ratio effects. However, the correlation is implemented using the hydraulic diameter for a rectangular channel:

$$Nu = 4.364 + \frac{0.086 \cdot \left(Re \cdot Pr \cdot \frac{D_h}{L}\right)^{1.33}}{1 + 0.1 \cdot Pr \cdot \left(Re \cdot \frac{D_h}{L}\right)^{0.83}} \qquad [-] \tag{2}$$

This correlation is valid in the range of $0.7 < Pr < 7$ or $RePrD_h/L < 33$ for $Pr > 7$. Keeping the temperature above 20 $^\circ C$, the Prandtl number is below 7. When dealing with Reynolds number under 450, the end of the channel has a hydrodynamically developed boundary layer, where a correlation by Shah and London [7] for parallel plate ducts is applicable.

Knowing the Nusselt number, the convective heat transfer coefficient is calculated by [5]:

$$h = \frac{Nu \cdot k_{fluid}}{D_h} \qquad \left[\frac{W}{m^2 K}\right] \tag{3}$$

3. Experiment

The fundamental principle of PLIF is to have a fluorescent dye in a fluid which get excited by light from a laser at a proper wavelength, and then re-emits the light at a longer wavelength during spontaneous transition from the excited state down to the ground state [8, 9]. The wavelength is longer because of energy losses in the excited state. Because of thermal quenching the luminescent intensity is reduced with increasing temperature [10]. In this experiment rhodamine B is used as the fluorescent dye as a continuous Argon-Ion laser with a 20° lens illuminates the flow with green light with a wavelength of 532 nm, where the absorption intensity in rhodamine B is high. This can be seen in figure 2 (a).

The fluorescence intensity for rhodamine B vary with about 2 $\%/K$ [11], which makes it suitable for temperature measurements. For rhodamine B the energy is re-emitted close the wavelength of orange light in the vicinity of 590 nm. The fluorescence is captured by a 1024x768 pixel charged coupled device (CCD) SVS-VISTEK 204F camera with a 590 nm filter and 60 mm Nikon lens. The fluorescence intensity, I, can be described by the following equation [9]:

$$I = I_0 \, A \, \phi \, \epsilon \, C \, \frac{\lambda_e}{\lambda_f} \qquad [-] \tag{4}$$

I_0 is the excitation intensity, A is the fraction of collected light, ϕ is the quantum yield, ϵ is the molar absorptivity, and C is the concentration of rhodamine B. λ_e and λ_f is the wave length of the excitation light and the fluorescence light, respectively.

A schematic drawing of the experimental setup is shown in figure 2 (b). The power input is applied from an electric heater through a copper rod. The laser sheet is applied from one side of the setup and the CCD camera is set to take pictures perpendicular to the laser sheet.

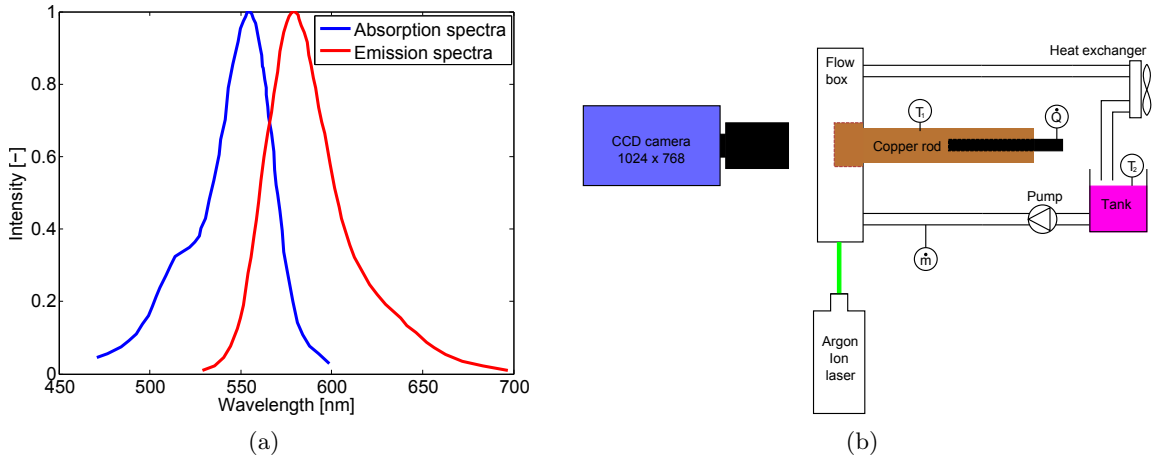

(a) (b)

Figure 2. *Figure (a) showing absorption and emission spectra of rhodamine B based on [12], and figure (b) showing schematic drawing of experimental setup.*

The correlation between the temperature and fluorescence intensity is evaluated to be linear [11]. To find this relationship the system is calibrated at steady state over a temperature

range of 30-55 $°C$. The CCD camera generates greyscale values corresponding to the different temperature values, hence making it possible to make the PLIF measurements.

The determination of the conventional Nusselt number is dependent on the Reynolds number, which is based on a flow measurement from a flow sensor, which is a FT-210 sensor from Gams with an accuracy of $\pm$ 3 %. The temperature in the copper rod is measured in order to approximate the fin temperature, as they are assumed equal, and the position is shown as T_1 in figure 2 (b). After the temperature experiments the calibration is again carried out with matching temperatures, in order to check for photobleach, described in the error analysis. At each measurement a total of 50 pictures is saved in TIFF-format with an exposure time of 1.7 s. The laser power is 1.2 W throughout the experiments.

To process the data a MATLAB algorithm is made for the present study. The 50 pictures from each measurement is averaged in order to reduce noise. A linear least squares fit is made between the greyscale values and the temperature. Each measured calibration temperature in each pixel is compared with the temperature calculated from the 1st order polynomial. If the deviation is more than 10 % the points are removed, and a new 1st order polynomial between the remaining points is made. The MATLAB image toolbox is used for faster data processing. The pixel size may be reduced for faster data processing, but it may also introduce an error in the resolution of the thermal boundary layer. Instead, only a section of the image is processed, speeding up calculation time.

The inlet area of the channels is distorted by reflections, and should not be considered. It is considered difficult to align a laser sheet accurately to a channel, because of laser spreading, and thus shadow effects occur. Hence, due to symmetry, only half of the channel width is considered, and may as well be enough for temperature gradient analysis. The fluid pixel intensities are averaged by the surrounding 5 pixels at the wall, and averaged with its surrounding 8 pixels elsewhere. This is in principle a low-pass filter, and reduces the pixel-to-pixel noise.

Figure 3 (a) shows a temperature plot of the averaged 50 calibration images at a temperature of 40.2 $°C$ based on the entire first calibration series. Consequently, the temperatures should be 40.2 $°C$ in the mini channels as each pixel is calibrated to fit this value. In figure 3 (a) the full sized image of the mini channels is shown from above, and the inlet of the water is from the right side of the image.

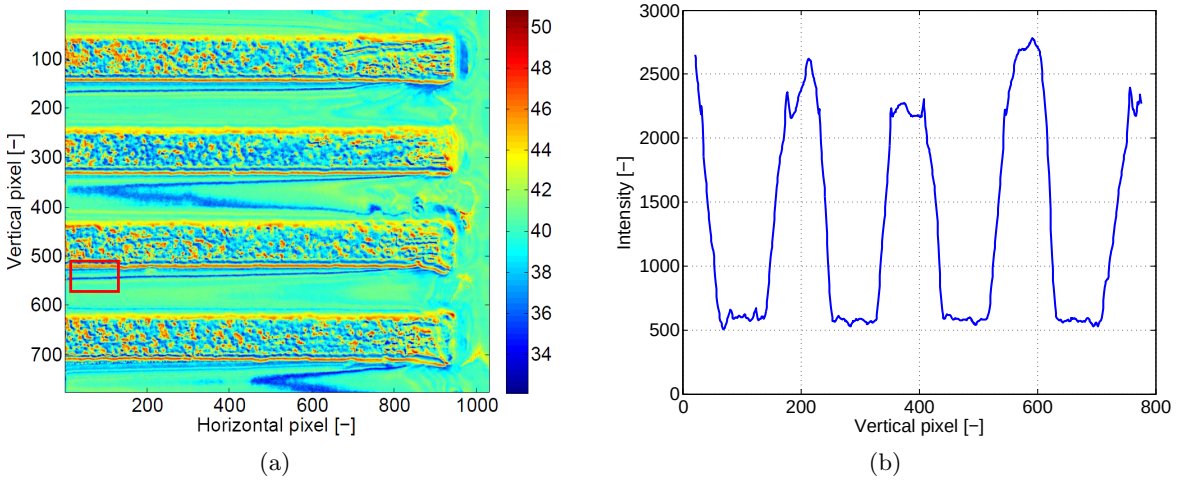

Figure 3. *Figure (a) showing temperature contour in the investigation area at calibrated temperature of 40.2 °C, and figure (b) showing intensity at a horizontal pixel value of 70.*

It can be seen in figure 3 (a) that the temperature is relatively uniform in the mini channels,

while the intensity varies significantly inside the wall. The temperature of the wall is forced to fit the measured copper rod temperature. An important thing is to consider where the boundary between the water and the wall is located, as the experimentally measured h-values highly depend on this assumption. In figure 3 (a) it is shown that some areas of the mini channels should be disregarded due to poor quality. The selected area of interest is determined to be from 5 to 120 for the horizontal pixels.

To determine which vertical pixels to investigate a plot of the intensities along a constant pixel value of 70 is shown in figure 3 (b). In this figure the high spikes of intensity are in the channels, while the lower spikes are inside the wall. The curve from the vertical pixels with a value of 500 to 625 is seen to the have the smoothest curve. The vertical pixels from 509 to 578 are selected for the area of interest, as only half of the mini channel is considered. The selected area of interest is the red square in figure 3 (a). This area is a small portion of the whole image, which is mainly because of less calculation time, but also because of unwanted disturbances in other areas. However, in the area of interest there is optical disturbances, represented by a line of lower temperature.

4. Results

Temperature results are shown in figure 4 (a) and (b). The area of investigation is 115 horizontal pixels and 69 vertical pixels resulting in 611 μm x 366 μm, showing half of the channel width. It is assumed that the temperature profile of the channel in the region of interest is symmetric along the center of the channel. Figure 4 (a) shows the temperature of the wall and fluid. The wall is set to a constant temperature of 57.8 $^{\circ}C$, which is the copper rod temperature. A temperature decrease occur perpendicular to the wall, as shown in figure 4 (b). The temperature decrease follows a parabolic tendency until 35-39 vertical pixels and is again parabolic after these points. The discontinuity is because of optical disturbances, which result in a line of lower temperature throughout the image in figure 4 (a).

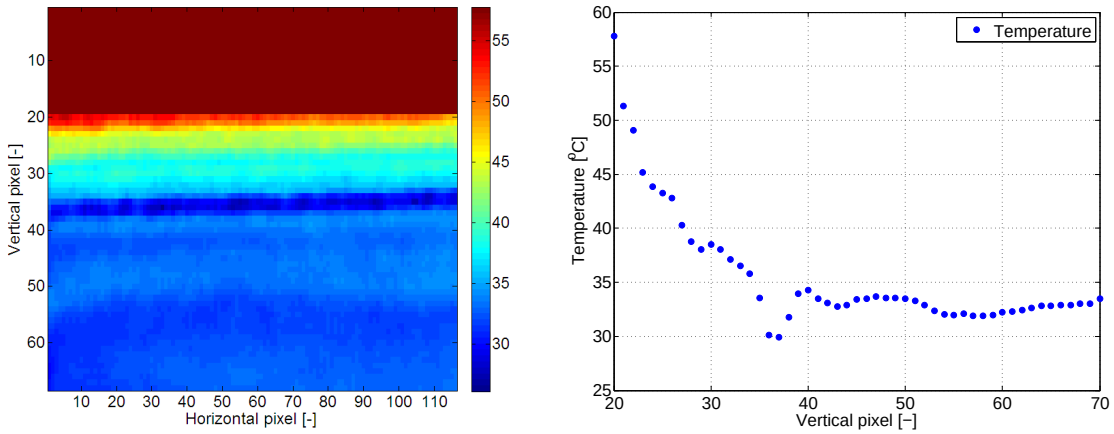

(a) (b)

Figure 4. *Figure (a) showing temperature contour in the selected area of interest, and figure (b) showing the vertical temperature profile at a horizontal pixel value of 70.*

Determination of the convective heat transfer coefficient, and hence the Nusselt number is carried out by evaluating the temperature gradient close to the wall using equation (1). Due to the no-slip condition, the fluid particle adjacent to the wall must be the same as the wall temperature. The PLIF experiment gives no information about the wall temperature, but the temperature is measured 25 mm from the top of the fin, and from thermal resistance theory the

fin temperature must be less than the measured temperature. Due to uncertainties of the thermal resistance analysis, the two perpendicular pixels adjacent to the wall is used for estimation of the temperature gradient. The pixel length is estimated to be 5.31 μm. The h-values calculated from the PLIF experiment is shown in figure 5. The mean h-value is 9,299 W/m^2K equivalent to a Nusselt number of 13.89. The calculated measured h-values are validated by the Stephan and Preusser Nusselt number approximation in the same region of interest, shown in figure 5. The mean conventional based h-value is 9,335 W/m^2K equivalent to a Nusselt number of 13.95.

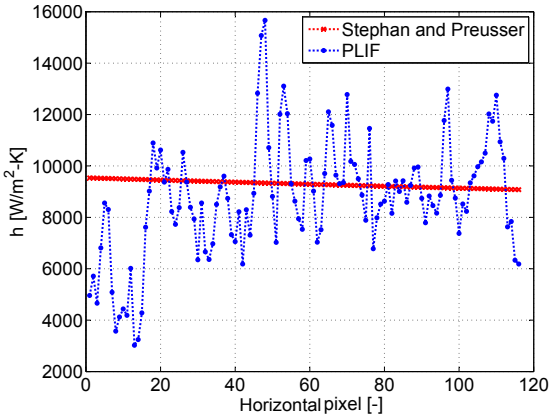

Figure 5. *Comparison of convective heat transfer coefficient based on conventional correlations and PLIF.*

5. Error Analysis

Errors and uncertainties encountered using PLIF are described by Coolen et al. [9] and Golnabi [13]. The main uncertainty is the calibration. The mapping of intensity to temperature is highly dependent on the curve fit from the calibration. It is important to reach steady state conditions, as a uniform temperature is needed. The temperature deviation in the tank water (T_2 in figure 2 (b)) is found sufficiently small, hence steady state is assumed.

An important factor influencing the emitted intensity is photobleaching of the dye. Photobleaching covers degradation of the dye as it is exposed to high power laser light, and results in a lower temperature due to less quantum yield [9], following equation (4).

A calibration between the temperature and the intensity is made before and after the experiments. The relative difference between the averaged calibration image for each of the calibration temperatures varies between 10.4 and 17.0 % for the fluid zone. Because of this difference an average between the two calibration sets is used for the making the 1st order polynomial fit between the temperatures and the intensity. A reason for the size of the relative difference could be that the temperature varied with $\pm$ 0.1 $^\circ C$ during the experiment making the calibration temperature diverge slighty from each other, but also that rhodamine B could be deposited in the setup during the experiment, or that photobleaching occurs. A method to avoid photobleaching could be to implement a mechanical shutter in front of the laser, as the time the dye is exposed to the laser between the experiments then could be reduced. Another method is to use a larger volume of water and dye, which also reduces the laser exposure time pr. rhodamine B molecule. The relative difference between the first and second calibration measurement at a temperature of 30.2 $^\circ C$ for the selected area of interest is shown in figure 6, where it can be seen that the relative difference is largest in the range of 0-20 vertical pixels, which is the wall. In the vicinity of the vertical pixel 36 the relative difference also increases due to optical disturbances, shown in figure 4 (a). For the rest of the selected area of investigation

the relative difference seems to be more constant. The overall relative difference between these two calibration images is 16.2 % for the fluid zone.

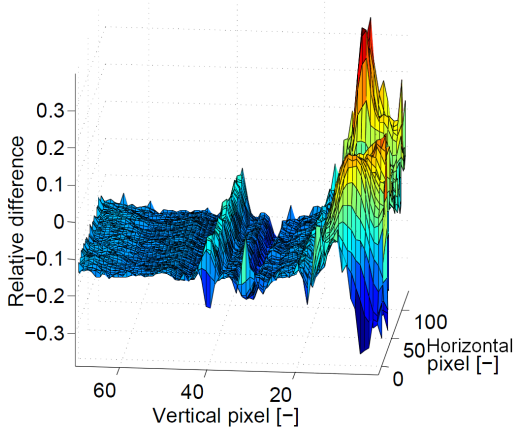

Figure 6. *Relative difference between first and second set of calibration images at a temperature of 30.2 °C.*

In figure 7 (a) a histogram of a random pixel (70,25) in figure 4 (a) is shown. The normal distribution of this histogram is also shown, and the sample mean is 1724. The standard deviation of 50 values in this pixel is found to be 74.3 which supports the choice of averaging over 50 pictures. With a 95 % confidence interval the deviation from the mean is calculated to be ± 20.6, which gives a deviation in temperature of ±1.2 %. In figure 7 (b) the calibration points in pixel (70,25) is shown with a linear fit resulting in a relative deviation of maximum 2 %. The assumption of a linear fit between intensity and temperature where tested at several pixels, and in the present work it is seen to match in the given temperature ranges.

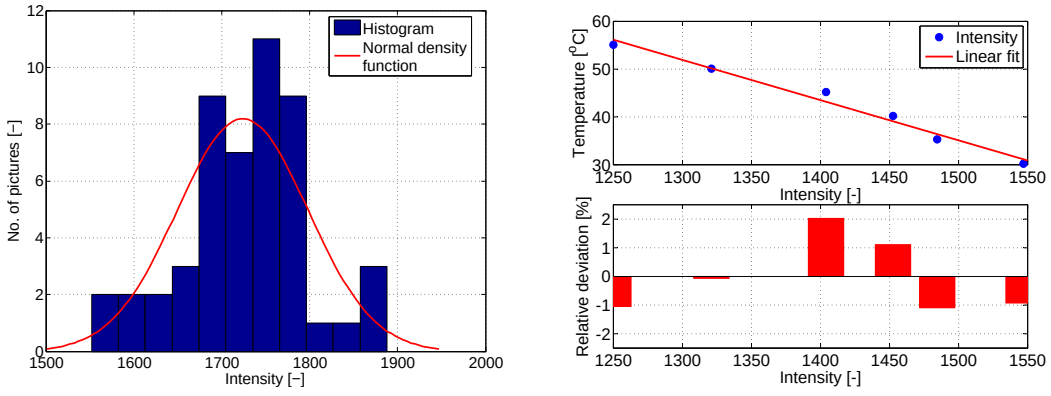

Figure 7. *Figure (a) showing histogram of pixel intensity for the 50 pictures in the temperature measurement with the histogram's normal distribution, and figure (b) showing calibration fit and accuracy.*

A source of error when using one-color PLIF is shadowgraph, described by Coolen et al. [9]. Shadowgraph occurs in areas of high temperature gradient due to local density variation causing a difference in the refractive index. Shadowgraph is significant when the temperature gradient in the direction of the laser light is more than 1 $°C/mm$. It is not seen to be the case in the

present study, due to a temperature difference in and out of the channel of approximately 0.05 $^{\circ}C/mm$, which is in the direction of the laser light. Also, the focus point of the CCD camera can induce errors, as it is hard to adjust this due to small length scales.

One of the main assumptions in the present paper is the determination of the wall boundary, as it may fall within a fraction of a pixel. If the wall boundary is misplaced it will introduce an error in the calculation of the convective heat transfer coefficient.

6. Conclusion

Heat transfer in mini channels with a hydraulic diameter of 889 μm is investigated experimentally using PLIF. With a Reynolds number of 260 the experimentally evaluated h-value is compared to a conventional correlation from Stephan and Preusser [6]. The applicability of PLIF is compared to the conventional correlation, and no significant difference is seen. The average resulting h-value for the investigated area is shown to be 9,299 W/m^2K for the experiment and 9,335 W/m^2K for the conventional correlation. The resolution of the temperature gradient is thus concluded to be sufficient, as in the present paper it is found advantageous not to downscale the picture resolution. However, a local heat transfer coefficient is not resolved precisely due to fluctuations.

Besides this, the applicability of PLIF over the whole geometry is not found satisfactory, as optical disturbances are found. The laser needs to be aligned properly to the channel of interest in order to avoid shadows, as this have a great importance on the accuracy of the experiment. Theoretically there is no lower limit on channel width in the experiment, as long as the laser and the camera are positioned properly. This is based on the fact, that in the present study approximately 11 μm of the channel width is used to find the h-value. The alignment of the laser influences the choice of the area of interest, because the intensity further downstream in the channel is limited. It is found important to accurately determine the wall position in the image, as the two pixels adjacent to the wall is used to calculate the h-value.

References

[1] Gao P, Person S L and Favre-Marinet M 2002 *Int. J. of Thermal Sciences* **41** 1017–1027

[2] Adams T M and Abdel-Khalik S I 1998 *Int. J. Heat Mass Transfer* **41** 851–857

[3] Rahman M M 2000 *Int. Comm. Heat Mass Transfer* **27** 495–506

[4] Qu W and Mudawar I 2002 *Int. J. Heat Mass Transfer* **45** 2549–2565

[5] Cengel Y A 2006 *Heat and Mass Transfer - A Practical Approach* 3rd ed (McGraw Hill)

[6] Stephan K and Preusser P 1979 *Chem. Ing. Tech.* **51** 37

[7] Shah R K and London A L 1978 *Advances in Heat Transfer - Laminar Flow Forced Convection in Ducts* (Academic Press)

[8] Dantec 2001 Flowmanager add-on: Plif-module Installation and Users guide publication no.: 9040U3651

[9] Coolen M C J, Kieft R N, Rindt C C M and van Steenhoven A A 1999 *Experiments in Fluids* **27** 420–426

[10] Liu T and Sullivan J 2005 *Pressure and Temperature Sensitive Paints* 1st ed (Springer)

[11] Sakakibara J, Hishida K and Maeda M 1993 *Experiments in Fluids* **16** 82–96

[12] Terpetschnig E, Povrozin Y and Eichorst J 2012 Polarization standards ISS, Inc http://www.iss.com

[13] Golnabi H 2006 *Optics & Laser Technology* **38** 152–161